ELSEVIER

Chemical Engineering Journal 82 (2001) 57–71

Chemical Engineering Journal

www.elsevier.com/locate/cej

Structured reactors for kinetic measurements in catalytic combustion

Gianpiero Groppi, Watari Ibashi[1], Enrico Tronconi, Pio Forzatti*

Dipartimento di Chimica Industriale e Ingegneria Chimica "G. Natta", Politecnico di Milano, 32, 20133 Milan, Italy

Received 1 June 2000; accepted 3 November 2000

Abstract

Two types of laboratory structured reactors, which closely resemble industrial monolith catalysts, are theoretically and experimentally investigated for measurements of catalytic combustion kinetics under severe conditions: the annular reactor, consisting of a ceramic tube externally coated with a thin catalyst layer and coaxially placed in a slightly larger quartz tube; and the metallic plate-type reactor, consisting of an assembled packet of metallic slabs coated with a ceramic catalytic layer.

After a brief description of an active coating deposition method suitable to provide structured reactors with adequate characteristics, a mathematical model analysis of the annular reactor aimed at the design of the optimal configuration for kinetic investigations is first presented. The resulting advantages, including: (i) negligible pressure drops; (ii) minimal impact of diffusional limitations in high temperature — high GHSV experiments; (iii) effective dissipation of reaction heat are then experimentally demonstrated for the case of CH_4 combustion over a $PdO/\gamma\text{-}Al_2O_3$ catalyst with high noble metal loading (10% w/w of Pd).

The feasibility of near-isothermal operation with the metallic plate-type reactor by an extremely effective dissipation of reaction heat through proper selection of highly conductive support materials and of the geometry of the metallic slabs is finally discussed and experimentally demonstrated for the case of combustion of CO at high concentrations over a $PdO/\gamma\text{-}Al_2O_3$ (3% w/w of Pd) catalyst.

Keywords: Kinetic measurements; Catalytic combustion; Structured catalysts; Calladium catalysts

1. Introduction

Catalytic combustion has been commercially applied for a long time to the elimination of organic compounds in the tail stream of combustion and industrial processes. Recently novel applications devoted to the production of heat and energy are coming to the market. Commercialization of catalytic combustors for gas turbines with ultra low emissions of NO_x CO and unburned hydrocarbons [1] has been started. The first commercial application of XONON technology by Catalytica [2,3] has been scheduled to be operational at the 750 MWe Pastoria Energy Facility in South California by the summer of 2003 [4]. Also domestic catalytic burners with NO_x emissions below 5 ppm [5] have been launched into the market. Besides several other catalytic combustion devices (premixed radiant burners, industrial boilers, cookers [6,7]) are currently under development both for domestic and industrial uses.

The industrial development of applications of catalytic combustion to the production of heat and energy poses several challenging problems both on the engineering and on the catalyst science side. Among these problems investigation of catalytic combustion kinetics under relevant conditions is a key issue [8,9]: on the applied side determination of reliable kinetic expressions is a major milestone in the development of mathematical models to be used for scale-up and design purposes; on a more fundamental side assessment of high temperature catalytic kinetics could provide insight into the role of the heterogeneous reactions under steady-state, ignited operations. Industrial applications of catalytic combustion for the production of heat and energy are typically extremely fast and strongly exothermic processes. Accordingly under relevant conditions diffusional limitations and marked temperature gradients can hardly be avoided which make laboratory kinetic measurements an arduous task. A short description of catalytic combustors for gas turbine applications would clarify this concept. In such devices the air exiting from the compressor at 10–20 atm and 300–450°C is preheated with a diffusive burner, accurately premixed with 2–4% of CH_4 (natural gas) and then fed to the catalyst. Within a residence time of few milliseconds, corresponding to a gas hourly space velocity (GHSV) in the order of

* Corresponding author. Tel.: +39-2-23993238; fax: +39-2-70638173.
E-mail address: pio.forzatti@polimi.it (P. Forzatti).
[1] On leave from Environmental Process Development Department, Industrial Machine & Plant Development Center, Ishikawajima-Harima Heavy Industries Co., Ltd., Yokohama, Japan.

1385-8947/01/$ – see front matter
PII: S1385-8947(00)00342-9

Nomenclature

C_f	concentration of f-species (mol/m^3)
$d_h = 2[r_0 - (r_i + \delta_w)]$	hydraulic diameter (m)
$Da = R_{CO} d_h / D_{CO} C_{CO}$	Damkohler number for CO combustion
$D_{ea,f}$	effective axial diffusivity of f-species (m^2/s)
$D_{e,f}$	effective intraporous diffusivity of f-species (m^2/s)
$D_{m,f}$	molecular diffusivity of f-species (m^2/s)
f	friction factor
$Gr = d_h^2 u / L D_{m,f}$	material Graetz number
$K_{g,f}$	mass transfer coefficient of f-species (m/s)
L	catalyst length (m)
n	catalyst layer coordinate (m)
P	pressure bar
P_f	partial pressure of the f-species (bar)
r_0	internal radius of the quartz tube (m)
r_i	external radius of the ceramic tube (m)
r_m	radius of macropores (m)
r_p	radius of micropores (m)
R_{CO}	rate of CO combustion (mol/m^2/s)
$Re = \rho u d_h / \mu$	Reynolds number
R_w	CH_4 combustion rate for catalyst unit volume (mol/m^3/s)
R'_w	CH_4 combustion rate for catalyst unit weight (mol/kg/s)
$Sh_f = K_{g,f} d_h / D_{m,f}$	Sherwood number of f-species
T	temperature (K)
u	axial gas velocity (m/s)
z	axial coordinate (m)

Greek letters

ρ	gas density (kg/m^3)
δ_A	size of the annular chamber (m)
δ_w	thickness of catalyst washcoat (m)
ϵ_m	volume fraction of macropores
ϵ_p	volume fraction of micropores
μ	gas viscosity (kg/m/s)
ν_f	stoichiometric coefficient of f-species

Subscripts

0	inlet condition
g	gas phase
w	catalyst layer

$10^7\ h^{-1}$ catalytic light-off must be achieved at temperatures as close as possible to those from the compressor air discharge to minimize diffusive burner pre-heating. Upon ignition the catalyst temperature increases up to 800–900°C so to heat the gas flow sufficiently to ignite gas phase combustion in the following homogeneous section. It is worth nothing that at this temperature the process is strongly affected, but due to turbulent flow in the monolith channels, not completely controlled by external diffusion so that catalytic kinetics could still play a role. This indicates that the 300–900°C temperature range and the 2–4% CH_4 concentration range should be relevant to kinetic investigations. Non-adiabatic applications such as industrial and domestic boilers are characterized by lower GHSV, but even higher fuel concentrations, e.g. radiant catalytic burners are typically operated with an equivalent ratio of 1.3, which corresponds to 7.3% of inlet CH_4 concentration, in order to minimize heat losses associated with the hot exhaust gases.

Another peculiar feature of catalytic combustion is that, due to the simultaneous presence of pressure drop and mass/heat transfer constraints, structured catalysts (monolith honeycombs and foams, fibrous panels) are typically used, whose properties could be significantly different from those of powder or grain catalysts used in conventional laboratory packed bed reactors.

On the other hand, structured catalytic reactors, which present strong analogies with the industrial catalysts, can be conceived and designed to obtain chemical kinetics data under extremely severe conditions. Along these lines McCarty [10] developed the annular reactor for investigation of high temperature kinetics of CH_4 combustion on PdO-based catalysts. This structured catalytic reactor consists of a ceramic tube coated with a thin catalyst layer and co-axially placed within a quartz tube to form an annular chamber where the gas flows straightforward. Although no quantitative analysis was reported, McCarty claimed that, using small annular gap distances (0.1–0.3 mm) and thin catalyst layers (10–40 μm), rate measurements were possible at high temperature with minimal thermal and concentration gradients across the gas boundary layer. A similar reactor configuration, but with larger size of the annular chamber and thicker catalyst layer, was adopted by Johansonn et al. [11] and by Beretta et al. [12]. The latter authors performed an engineering analysis of the annular reactor claiming the following advantages: (i) possibility to achieve very high GHSV with negligible pressure drops; (ii) possibility to maintain partial conversion at high temperature; (iii) well defined geometry (and gas flow pattern) that allows one to take into account diffusion effects; (iv) effective dissipation of reaction heat through radiation from the catalyst skin. Taking advantage of these features, a kinetic investigation of CO combustion over Mn-substituted hexaaluminates was performed. However, the data were markedly affected by external diffusion, which was taken into account through experimental determination of the mass transfer coefficient [12]. With respect to the onset of marked temperature gradients

associated with the strongly exothermic combustion, another structured reactor concept can be effectively exploited. By means of mathematical model simulation of a multitubular reactor for highly exothermic processes Groppi and Tronconi [13] theoretically demonstrated the capability of metallic monolith catalysts to secure an extremely efficient dissipation of reaction heat through a proper choice of support material and monolith geometry. This result can be scaled down to laboratory reactors for kinetic measurements by assembling packets of highly conductive metallic slabs coated with thin catalyst layer in a plate-type parallel-passage reactor configuration. Such a concept has been recently, demonstrated experimentally [14].

In this paper the potential of the annular and of the metallic plate-type reactors for investigation of catalytic combustion kinetics over very active PdO/γ-Al_2O_3 catalysts will be addressed. First a washcoating technique which allows to deposit active layers with suitable geometrical, morphological and catalytic properties onto metallic and ceramic structured supports will be described. Concerning the annular reactor, the design optimization by modeling analysis, aimed at minimizing diffusional effects, will be illustrated, and kinetic data on high temperature CH_4 combustion will be presented. Concerning the metallic plate-type reactor, the effects of the support material and of the slab geometry on the heat transfer properties will be discussed, and kinetic data for combustion of CO at high concentrations will be finally presented.

2. Experimental

2.1. Deposition of the catalyst layer

To prepare structured reactors suitable for kinetic investigation a coating technique must be developed which allows one to deposit onto ceramic and metallic supports active catalyst layers with the following characteristics: (i) good adhesion properties which resist under reacting conditions; (ii) morphological and activity properties which resemble those of industrial catalysts; (iii) uniform thickness which can be controlled through preparation parameters.

In this work a washcoating procedure partially derived from patent indications [15–17] has been adopted. The washcoat was deposited according to the following two steps: (a) deposition of a pseudo-bohemite primer, prepared by dispersing 10% (w/w) of a commercial pseudo-bohemite (Disperal, supplied by Condea Chemie) in a 0.4% (w/w) HNO_3 solution; the supports were then dipped into the aluminum hydroxide gel and dried at room temperature for 4–5 h; (b) deposition of the PdO/γ-Al_2O_3 washcoat: in this second stage a catalytic powder prepared via dry impregnation with a $Pd(NO_3)_2$ solution (Aldrich) of a γ-Al_2O_3 with particle size $<0.1\,\mu m$ was suspended in a HNO_3 aqueous solution. The catalytic slurry was vigorously stirred for (16 h) in order to obtain a gel-like suspension. The primerized supports were then dipped and flash heated at 280°C.

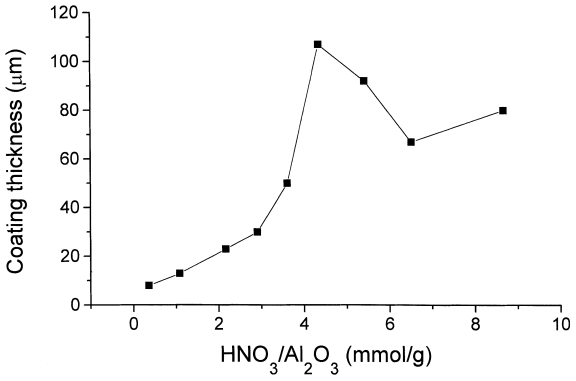

Fig. 1. Effect of HNO_3 concentration in the slurry on the thickness of the deposited γ-Al_2O_3 layer.

The procedure above was tested over several metallic foils (aluminum, AISI 304 steel, FeCr alloy and copper) and over α-Al_2O_3 ceramic tubes. SEM micrographs and ultrasounds tests [15] evidenced good uniformity and adhesion properties of the catalytic layer. The active coating exhibited morphological and catalytic properties close to those of the starting catalytic powders. CO catalytic combustion tests performed with a packed bed filled with catalyst powder and with a structured metallic plate-type reactor provided the same CO_2 productivity at given temperature and CO feed concentration [19]. Measurements performed by N_2 adsorption at 77 K (CarloErba Sorptomatic 1900 series) on a granular sample, obtained by scratching a flash-heated coating, provided a surface area of $110\,m^2/g$. Porosity measurements by Hg penetration performed on the same sample provided a pore volume of $0.48\,cm^3/g$ with an average pore radius of 80 Å. Such a porosity appears slightly low when compared with the coating density of $\approx 1\,g/cm^3$ calculated on the basis of independent thickness (SEM) and weight measurements. Assuming a skeletal density of $3.5\,g/cm^3$ for γ-Al_2O_3 [18] an additional pore volume of about $0.2\,cm^3/g$ is expected. Such a pore volume could be associated with both micropores, scarcely accessible to the reactants, and macropores that, on the other hand, could enhance the intraphase diffusion rate. In the absence of direct evidence for such a macropore fraction, its contribution has been neglected in the simulation below in order to obtain a conservative estimate of the intraphase diffusion resistances.

An extensive investigation has been also performed on the effect of several parameters of the deposition procedure (water and HNO_3 concentrations in the slurry, withdrawal speed of the coated sample from the slurry) on the properties of the active layers. In Fig. 1, the effect of HNO_3 concentration in the slurry, identified as the most critical parameter, on the layer thickness is reported. Data in Fig. 1, which refers to a pure γ-Al_2O_3 slurry, show that in the 0.3–2.9 mmol/g HNO_3 concentration range the layer thickness slightly increases from 8 to 30 μm. Above these concentrations the layer thickness rapidly increases, passes through a

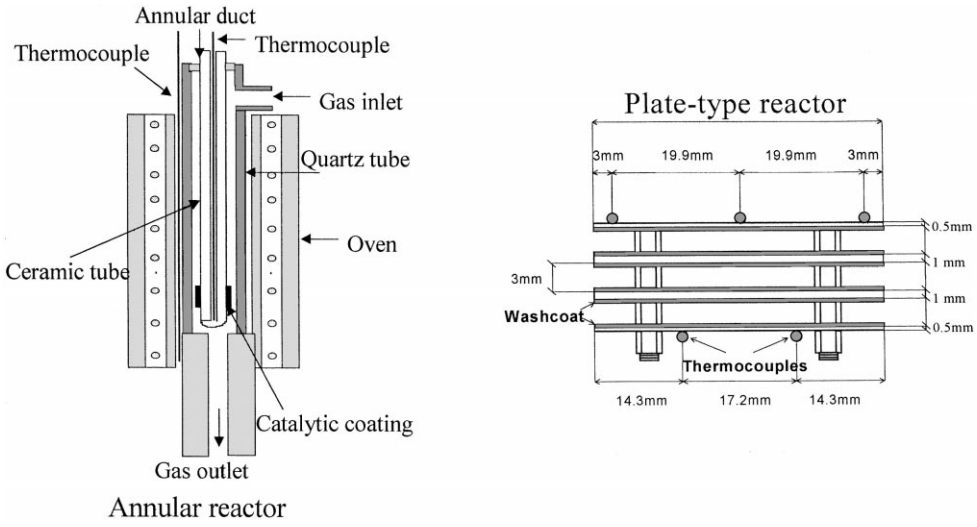

Fig. 2. Schematic of the investigated structured catalytic reactors.

maximum and then gradually decreases. Good adhesion properties have only been obtained for HNO_3 concentrations below 3.6 mmole/g-Al_2O_3 i.e. for catalyst layers thinner than 50 μm.

The data above have clearly demonstrated that, through proper selection of the parameters of the deposition procedure, uniform active layers as thin as 5–10 μm can be obtained which are well adherent and exhibit suitable morphological and catalytic properties.

2.2. Structured reactors

Fig. 2a,b reports the schematics of the two investigated structured reactors. The annular reactor (Fig. 2a) consists of an internal α-Al_2O_3 ceramic tube coaxially placed in an external quartz tube. The gas flows downwards in the annulus between the ceramic and the quartz tubes. The PdO/γ-Al_2O_3 (Pd = 10% w/w) catalyst is deposited on the external surface of the ceramic tube, near the bottom of the annular duct to enhance pre-heating of the gas phase. The bottom of the ceramic tube is sealed with thermal cement to avoid gas leakage. The reactor is placed vertically in an electric oven (Tersid MTF 10/25) and is equipped with two sliding thermocouples. The one placed inside the internal cavity of the α-Al_2O_3 tube allows one to measure the axial temperature profile of the catalyst, assuming thermal equilibrium across the transverse section of the ceramic tube. The other one is placed in a quartz well cemented to the external wall of the quartz tube: measurements of temperature profiles from this external thermocouple have been used to check the consistency of the enthalpy balance.

In the case of the metallic plate-type reactor (Fig. 2b), the catalyst consisted of four slabs (width = 46 mm, length = 200 mm), which were coated with PdO/γ-Al_2O_3 (Pd = 3% w/w, total coating load = 3.84 g) and assembled with spacers 3 mm apart in order to form three parallel rectangular channels. The slabs were made of aluminum (99.5% commercial purity), with thickness of the two central slabs = 1 mm, and thickness of the two outer slabs = 0.5 mm, since these were coated with catalyst on one side only. The plate-type catalyst was eventually equipped with five 1/16 in. stainless steel tubes at different transverse locations, acting as thermowells for sliding J-type thermocouples, and loaded into a stainless steel reactor tube (46 mm × 26 mm internal cross section) placed inside an oven with air recirculation (Mazzali Thermotest), which secured an uniform external temperature distribution. The T-profiles along the upper and lower external reactor walls were also monitored by two sliding thermocouples. The pressure drop in the reactor was negligible in all runs.

2.3. Kinetic tests

In both CH_4 and CO combustion tests analysis of reactants and products was performed by an online GC (HP 6890 Series) equipped with a Porapak Q and a 5 Å molecular sieve 3 m long packed columns with an in series TCD detector. Carbon balance of all the considered runs were within ±5%.

The targeted flow rate and feed composition was obtained with electronic mass flow controllers (Brooks 5850 TR series). Test conditions were widely varied depending on the reactor configuration and will be given in details in the following sections.

3. Results and discussion

3.1. Design of the annular reactor

3.1.1. Mathematical model

As stated above the use of annular reactors for kinetic measurements in catalytic combustion has been already reported in the literature [10–12]. However, no specific efforts

have been devoted to the design of a reactor configuration targeted to minimize the impact of diffusional limitations on kinetic data. Taking advantage of the well defined geometry of the annular reactor this task can be nicely performed through classical design tools of chemical engineering. Along these lines, a mathematical model of the annular catalytic reactor has been developed under the following assumptions: (i) one-dimensional lumped description of the gas phase and two-dimensional distributed description of the catalyst phase; (ii) fully developed laminar flow in the annulus; (iii) steady-state conditions; (iv) isothermal catalyst and gas phase; (v) negligible pressure drop; (vi) planar geometry of the active washcoat in view of the high ratio of ceramic tube radius to catalyst thickness ($r_i/\delta_w > 50$).

In order to account for all the possible "mass transfer noises" on kinetics, the contributions of gas–solid external diffusion, axial diffusion in the gas phase, internal diffusion in the catalyst phase have been included. The model consists of the following mass-balance equations for the gas and catalyst phase:

f-species mass balances (f = CH_4, H_2O)

$$u\frac{\partial C_{f,g}}{\partial z} = D_{ea,f}\frac{\partial^2 C_{f,g}}{\partial z^2} - \frac{4}{d_h}\left[\frac{(r_i+\delta_w)}{r_0+(r_i+\delta_w)}\right] K_{g,f}(C_{f,g}-C_{f,w}) \quad \text{(gas phase)} \tag{1}$$

$$D_{e,f}\frac{\partial^2 C_{f,w}}{\partial n^2} + \nu_f R_w = 0 \quad \text{(catalyst phase)} \tag{2}$$

Boundary conditions:

$$u(C_{f,g}-C^0_{f,g}) = D_{ea,f}\frac{\partial C_{f,g}}{\partial z} \qquad (\text{at } z=0) \tag{3}$$

$$\frac{\partial C_{f,g}}{\partial z} = 0 \qquad (\text{at } z=L) \tag{4}$$

$$D_{e,f}\frac{\partial C_{f,w}}{\partial n} = K_{g,f}(C_{f,g}-C_{f,w}) \quad (\text{at g/w interface } n=\delta_w) \tag{5}$$

$$\frac{\partial C_{f,w}}{\partial n} = 0 \qquad (\text{at catalyst/}\alpha\text{-}Al_2O_3\text{ interface } n=0) \tag{6}$$

The PDEs (1)–(6) have been solved numerically in dimensionless form. Orthogonal collocations on finite elements [20] with third-order polynomials in each element have been used for discretization of concentration profiles along the axial direction, whereas orthogonal collocations [20] have been used for discretization of internal concentration profiles in the catalyst thickness. The resulting set of AEs has been solved by a continuation method [21]. Seven elements with constant mesh along the axial direction and four collocation points along the normal direction have been required to achieve numerical convergence.

The design of the annular reactor has been performed by simulating CH_4 lean combustion tests over a very active PdO-based catalyst under conditions which typically correspond to very fast reactions, i.e. high temperature (600°C) with a water-free feed. Pressure has been set to 1 bar in line with the assumption of negligible pressure drop.

The following kinetic expression has been adopted for methane combustion over Pd-based catalysts:

$$R_w = \left(\frac{K_r C_{CH_4,w}}{1+K_{H_2O}C_{H_2O,w}}\right) \ (\text{mol/m}^3\text{s}) \tag{7}$$

On the basis of literature indications, which report reaction orders of 1, 0 and −1 in CH_4, O_2 and H_2O concentration, respectively [22,23], the LHHW-type rate (Eq. (7)) has been adopted instead of power law expressions proposed in the literature to avoid numerical problems at the catalyst inlet. Kinetic parameters have been tuned through preliminary combustion experiments as to simulate a very fast reaction providing 60% conversion at 600°C, GHSV = $3\times10^6\ \text{h}^{-1}$, with a water free feed.

The physical properties of the gas phase have been calculated assuming ideal gas behavior and using the Fuller method [24] for evaluation of density and of molecular diffusion, respectively. The axial diffusion coefficient has been corrected to account for the additional dispersion associated with the laminar velocity profile in the 1D description of the gas phase [25]. However such a correction has been found to be negligible (less than 1%) at the simulated conditions.

Two types of catalyst morphology have been considered to assess the effect of intraporous diffusion: (i) one mono-modal pore size distribution, that has been derived from porosity measurements on the commercial γ-Al_2O_3 available in our lab for coating purposes neglecting any possible contribution of macropores in order to obtain a conservative estimate of the internal diffusion resistances; one bimodal pore size distribution with a significant macropore fraction and enhanced effective internal diffusion coefficients which have been calculated according to the Wakao and Smith model [26].

Sherwood numbers for calculation of external mass transfer coefficients have been derived from the heat transfer literature [27] on the basis of the analogy with the Graetz thermal problem, for an annular geometry with r_i/r_0 ratio close to one and with one adiabatic wall corresponding to zero mass flux condition at the quartz wall. Entrance effects have been neglected assuming a constant value of *Sh*. In fact the velocity profile is completely developed at the inlet of the catalytic zone of the annulus. Also concentration profiles can be considered fully developed being the material Graetz number ($Gr = d_h^2 u/LD_{m,f}$) lower than one [27].

The set of model parameters used in the reactor design analysis are summarized in Table 1.

In the simulations the radius of the quartz tube and the length of the catalyst bed have been taken as constant, whereas the radius of the ceramic tube and the thickness of the catalyst layer have been varied as design parameters of the reactor geometry.

Table 1
Simulation parameters for the annular reactor

Sh_∞	5.385	
Kinetics		
K_r (s^{-1})	3.992×10^3	
K_{H_2O} (m^3/mol)	3.509	
Catalyst morphology		
Pore distribution	$D_{e,f}^{CH_4}$ (m^2/s)	$D_{e,f}^{H_2O}$ (m^2/s) H_2O
Monomodal: $\epsilon_p = 0.5225$, $r_p = 9$ nm	1.102×10^{-6}	1.042×10^{-6}
Bimodal: $\epsilon_p = 0.5225$, $r_p = 9$ nm, $\epsilon_m = 0.1$, $r_m = 100$ nm	3.060×10^{-6}	2.909×10^{-6}
Gas properties		
$D_{m,f}$ (m^2/s)	CH_4	H_2O
	3.379×10^{-4}	3.826×10^{-4}
Operating conditions		
Flow rate (cm^3/s at STP)	1.67	
T (K)	873	
P (bar)	1	
O_2 (%, v/v)	20	
CH_4 (%, v/v)	0.75	
He	Balance	
Geometry		
L (m)	1.0×10^{-2}	
r_0 (m)	3.50×10^{-3}	

3.1.2. Simulation results

The following functions have been selected as design targets.

1. The average internal effectiveness factor, calculated according to:

$$\eta_{int}^{av} = \int_0^L \frac{\int_0^{\delta_w} R_w(z, n)\, dn}{R_w(z, \delta_w)} \frac{dz}{L} \tag{8}$$

which is an index of the global impact of intraporous diffusion.

2. The global effectiveness factor, defined as

$$\eta_{glob} = \frac{K_r^{eff}}{K_r}, \tag{9}$$

i.e. the ratio to the actual kinetic constant, K_r, of the pseudo-reaction rate constant K_r^{eff} that must be included in the following simple mathematical model of the annular reactor to calculate the same CH_4 conversion provided by the more complex model described above:

$$u \frac{dC_{f,g}}{dz} = \frac{(r_i + \delta_w)^2 - r_i^2}{r_0^2 - (r_i + \delta_w)^2} \nu_f R_w^{eff} \tag{10}$$

$$C_{f,g} = C_{f,g}^0 \quad (\text{at } z = 0) \tag{11}$$

with

$$R_w^{eff} = \left(\frac{K_r^{eff} C_{CH_4,w}}{1 + K_{H_2O} C_{H_2O,w}} \right) \ (\text{mol/m}^3\text{s}) \tag{12}$$

Such a simple model does not include any effect of diffusion on reaction rate, so that η_{glob} corresponds to the relative error associated with the analysis of conversion data when neglecting any diffusional phenomena, including internal, external gas–solid and gas phase axial diffusion. This appears as a more convenient index to describe the reactor performances than the classical effectiveness factor that accounts only for the internal and the external gas–solid diffusion. In Fig. 3a–d are reported the simulated contour lines of the average internal (Fig. 3a and c) and the global effectiveness factor (Fig. 3b and d) in catalyst thickness – size of the annular chamber ($\delta_w - \delta_a$) plane. Simulation results plotted in Fig. 3a, b and c, d refer to monomodal and bimodal pore distributions (see Table 1), respectively.

Fig. 3a shows that with a monomodal distribution of small mesopores internal diffusion becomes rapidly critical on increasing the catalyst thickness. Average internal effectiveness factors lower than 0.75 have been calculated with $\delta_w = 20\ \mu$m, and catalyst thickness must be kept as low as 10 μm to achieve η_{int}^{av} of about 0.9.

Comparison of Fig. 3b with Fig. 3a shows that in the investigated range of geometrical parameters the global effectiveness factor is only slightly lower than the internal one. This demonstrates that internal diffusion is the most critical phenomenon when keeping the size of the annular chamber reasonably small. However some effect of external gas diffusion can be observed as evidenced by the negative slope of the contour lines of global efficiencies on increasing δ_A. Such a negative slope could be associated both with the external gas–solid mass transfer rate, that obviously decreases on enlarging the annulus, and with the axial diffusion. Indeed at constant molar flow rate the actual gas velocity decreases on increasing δ_A so that the inhibiting effect associated with backward diffusion of H_2O produced in the reaction becomes of growing importance. Noteworthy

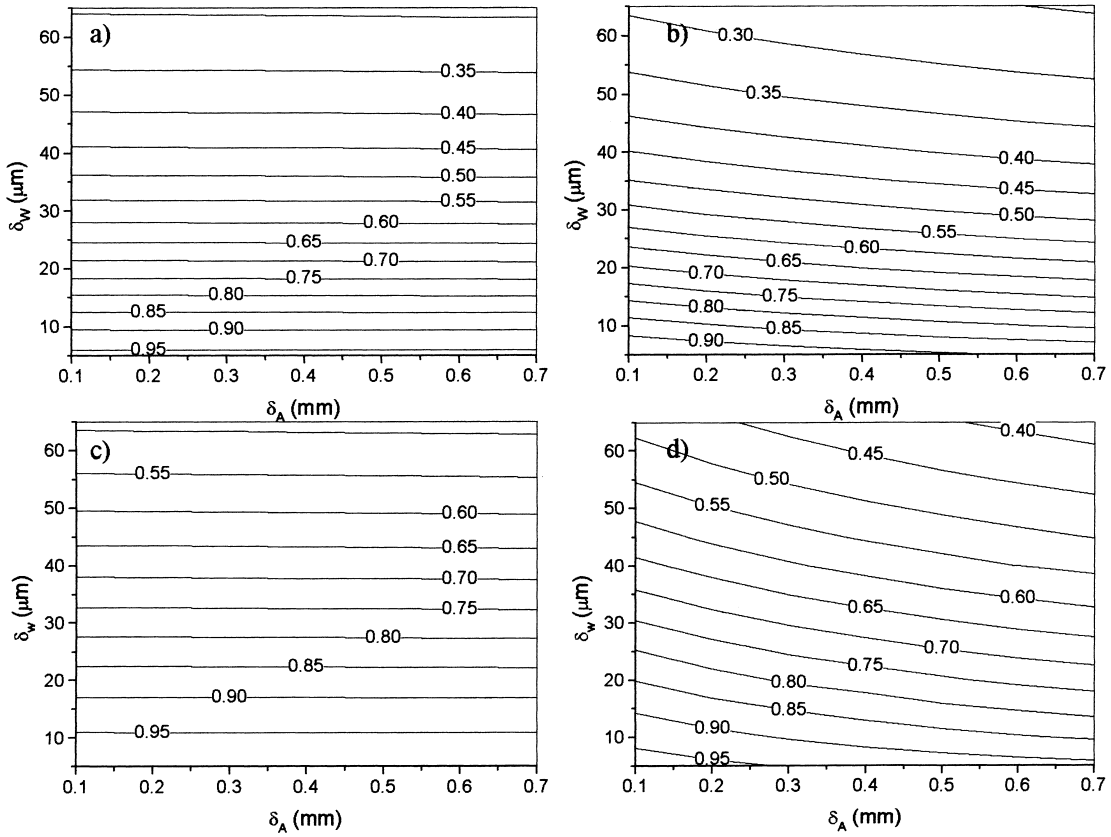

Fig. 3. Calculated contour lines of internal and global effectiveness factor with different catalyst morphologies in the $\delta_a - \delta_w$ plane: (a) η_{int} with monomodal pore distribution; (b) η_{glob} with monomodal pore distribution; (c) η_{int} with bimodal pore distribution; (d) η_{glob} with bimodal pore distribution.

simulations performed by setting $D_{ea,f} = 0$, i.e. neglecting the effect of axial diffusion, provide η_{glob} very close to the value of the internal effectiveness factor indicating the axial backward diffusion of H_2O as the main responsible for the decrease of external effectiveness factor (e.g. with $\delta_w = 10\,\mu m$ and $\delta_A = 0.5\,mm$; $\eta_{glob} = 0.8112$ and $\eta_{glob} = 0.8734$ have been calculated by neglecting and considering axial diffusion, to be compared with $\eta_{int}^{av} = 0.8916$).

The above results identify internal diffusion as the phenomenon governing the global catalyst effectiveness factor. Accordingly significant advantages could be obtained through deposition of active layers that exhibit a bimodal pore size distribution with a significant fraction of macropores, which warrants higher values of the effective diffusion coefficients. Comparison of Fig. 3c with Fig. 3a, clearly illustrates this point: with the bimodal pore distribution average internal efficiencies above 95% are calculated for $\delta_w = 10\,\mu m$ and thicker washcoats up to 20 μm still provide about 90% η_{int}^{av}. Fig. 3d shows that, due to the increase of internal diffusion rate, gas phase diffusion plays a more important, but still minor role in determining the global effectiveness factor. In fact steeper negative slopes of the contour line are obtained with respect to those observed in Fig. 3b. However the global effectiveness factors are still quite close to the corresponding η_{int}^{av}.

Considering the difficulties associated with the precise assessment of the porous texture and, even more, of the effective internal diffusion coefficient a conservative reactor design with $\delta_w = 10\,\mu m$ and $\delta_A = 0.25\,mm$ have been derived from the above results as a reasonable (also from the point of view of mechanical construction) configuration to minimize the impact of diffusional phenomena. It is worth stressing that the calculated 10% error associated with neglecting diffusion in such a reactor configuration is of the same order of the experimental error associated with conversion measurements with ±5% accuracy.

3.2. Experimental performances of the annular re actor

3.2.1. Pressure drop, role of homogeneous reaction and thermal behavior

The reactor configuration above was first tested with N_2 gas flow in order to check the pressure drop performances. In Fig. 4 the experimental data obtained with a flow rate of 400 cm^3/min STP, which corresponds to an actual linear gas velocity of 2.5–5 m/s depending on temperature and pressure, are compared with the pressure drop calculated according to the classical literature formula [27]:

$$\Delta P = \int_0^L \rho \left(u \frac{du}{dz} + f \frac{u^2}{\delta_A} \right) dz, \quad f = \frac{24}{Re} \left(\frac{r_i}{r_0} \right)^{0.035} \quad (13)$$

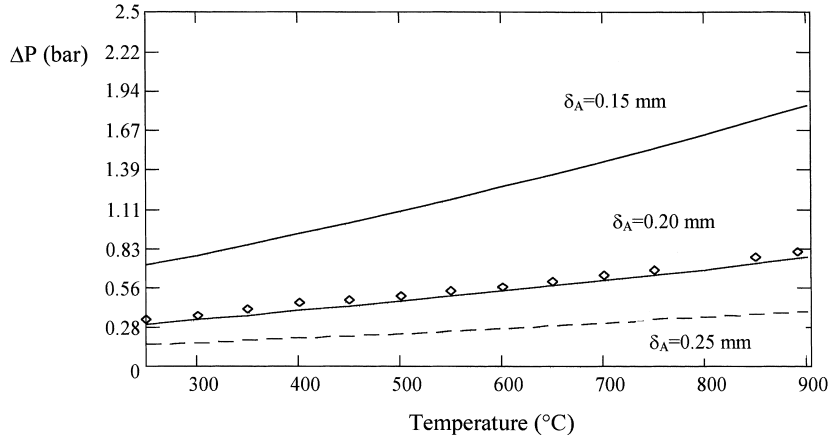

Fig. 4. Comparison of calculated and experimental pressure drops in the annular reactor. Flow rate: 400 cc/min at STP.

where inlet effects have been neglected (constant friction factor), but a differential formula has been used in order to take into account the effect of the experimental temperature profile on gas density (calculated assuming ideal gas behavior) and velocity (derived from continuity equation). Experimental data in Fig. 4 show that low, but not negligible pressure drops have occurred under such high flow rate conditions. Such pressure drops are accurately fitted using an annulus size that deviates from the design value well within the construction tolerance (0.2 versus 0.25 mm). This has been taken as an evidence that no particular modification from the design configuration, such as strong annulus eccentricity, has occurred. However it is worth noting that pressure drops as high as 0.5 bar observed at high temperature could be critical for detailed kinetic investigations. Besides this, result indicate that smaller annular chambers would provide some benefits with respect to diffusion limitations, but would result in serious pressure drop problems. On the other hand, with the actual catalyst load of 2 mg corresponding to the design configuration, a flow rate of 400 cm^3/min STP corresponds to GHSV higher than 10^7 cc/(g h) so that it can be significantly decreased without seriously affecting the possibility to collect kinetic data on very fast reactions. Accordingly experiments with N_2 flow rate of 100 cm^3/min STP have been performed showing negligible pressure drops in all the investigated temperature range. Such a flow rate, corresponding to GHSV $= 3 \times 10^6$ cc/(g h), has been then adopted in all the following kinetic experiments.

With such a flow rate blank experiments have been performed using an uncoated dense α-Al_2O_3 tube. The reactor has been fed with 0.8% of CH_4 in air and the oven temperature has been varied in order to gradually increase the maximum temperature measured by the internal thermocouple at the bottom of the ceramic tube up to 900°C. No CH_4 conversion has been detected up to 850°C and reacted CH_4 has remained below 10% also at 900°C. This indicates that the contribution of catalytic combustion over α-Al_2O_3 as well as the contribution of homogeneous reactions can be neglected in all the relevant temperature range. It is worth noting that the high surface to volume ratio associated with the small size of the annulus can play a significant role in quenching the homogeneous reaction. Indeed a similar effect was claimed to allow safe handling of inflammable H_2/O_2 mixtures in microstructured reactors with small channels of 140×200 μm size [28], i.e. of the same order of those of the annular reactor herein proposed.

Beretta et al. [12,29] have also investigated the behavior of the catalyst temperature profiles during CO combustion in an annular reactor with thicker catalyst layer ($\delta_w =$ 50–150 μm) and larger annular chamber ($\delta_A = 1.125$ mm), pointing out that radiation through the external catalyst skin is a quite effective mechanism for heat dissipation. The thermal behavior has been further investigated for the specific reactor configuration adopted in this work. Detailed results will be reported in a forthcoming paper [29], however a brief summary is given in Fig. 5, where the following

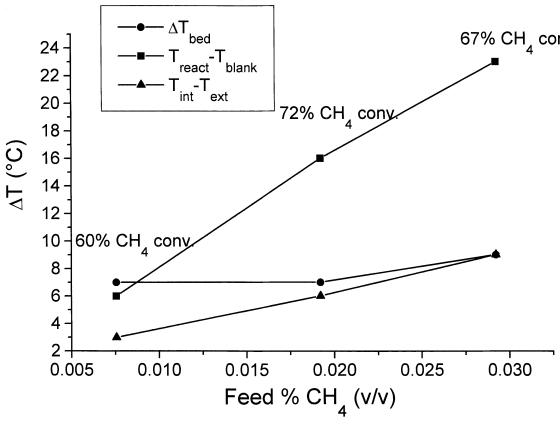

Fig. 5. Experimental temperature differences in the annular reactor during CH_4 combustion tests. $T_{react} - T_{blank}$: maximum difference between axial temperature profiles during reaction and blank experiments performed at the same flow rate and oven temperature; $T_{int} - T_{ext}$: maximum difference between axial temperature profiles measured under reaction by the internal and the external thermocouple; ΔT_{bed}: maximum temperature difference along the catalyst bed as measured by the internal thermocouple.

experimental temperature differences are plotted as functions of the inlet CH_4 concentration: (i) maximum difference between axial temperature profiles during reaction and blank experiments performed at the same flow rate and oven temperature ($T_{react} - T_{blank}$); (ii) maximum difference between axial temperature profiles measured under reaction by the internal and the external thermocouple ($T_{int} - T_{ext}$); (iii) maximum temperature difference along the catalyst bed as measured by the internal thermocouple (ΔT_{bed}). The first difference is an index of heat build up in the catalyst bed as a balance between heat of combustion and heat dissipation via all the possible mechanisms (radiation, convection and conduction). It gradually increases with CH_4 inlet concentration as a result of the enhanced combustion heat, however such an increase is very limited with respect to the corresponding increment of adiabatic temperature rise. This is due to the parallel enhancement of heat dissipation, that can be inferred from the increased difference between the temperatures of the catalyst and of the external wall of the quartz tube. The mechanism of effective heat dissipation has been investigated by both theoretical and experimental methods [30]. Calculations show that heat conduction through the ceramic tube can be neglected. On the other hand, CO combustion tests at temperatures ranging between 250–600°C have shown that both convection and radiation are effective heat dissipation mechanisms for the investigated configuration. Convection, which is quite effective due to the very small size of the annulus, plays a major role at low temperature. Radiation is of growing importance on increasing the temperature and becomes the dominant mechanism at 600°C. As a result, catalyst temperature profiles during CH_4 combustion at 600°C are maintained quite flat with an overall temperature difference along the catalyst bed below 10°C (Fig. 5). It is worth noting that nearly isothermal conditions have been obtained under more severe conditions than those reported by Beretta et al. [29] (3% CH_4 versus 3.5% CO). The main reason for this is that, thanks to the minimum amount of catalyst used in the annular reactor herein described, extremely high GHSV are achieved with a flow rate of 100 cm^3/min (STP) only, which is about one order of magnitude lower than those adopted by Beretta et al.. In fact at fixed fuel conversion and concentration the rate of heat production increases linearly with flow rate, whereas under laminar flow conditions, which actually prevail in the reactor, heat dissipation depends only on the reactor geometry.

Finally, it is worth pointing out that, as demonstrated by preliminary catalytic combustion experiments, partial CH_4 conversions could be achieved up to 600°C over a very active PdO/γ-Al_2O_3 catalyst with 10% (w/w) of Pd, thus making possible to collect kinetic data under conditions which were not previously explored.

3.2.2. Kinetic measurements in CH_4 combustion

On the basis of the above results an extended kinetic study of CH_4 combustion over the PdO/γ-Al_2O_3 catalyst with high metal loading has been then attempted in the following variable range: T = 400–600°C; H_2O_{in} = 0–9% (v/v), CH_{4in} = 0.8–3% (v/v), O_{2in} = 5–20% (v/v), He to balance; GHSV = 3×10^6 cm^3/(g h). Deactivation problems prevent to obtain well defined kinetics. In fact catalyst deactivation has been observed under reaction conditions: the CH_4 conversion measured in repeated standard tests (T = 500°C; H_2O_{in} = 0% (v/v), CH_{4in} = 0.8% (v/v), O_{2in} = 20% (v/v) decrease from 50 to 35% after 50 h time on stream (first phase) and decrease further to 30% after 200 h (second phase). Within the scope of this work, i.e. the demonstration of the reactor performances and not a detailed investigation of the catalyst behavior, the catalyst activity has been considered constant in the following kinetic analysis based on data collected in the second phase within a range of 20–30 h time of stream.

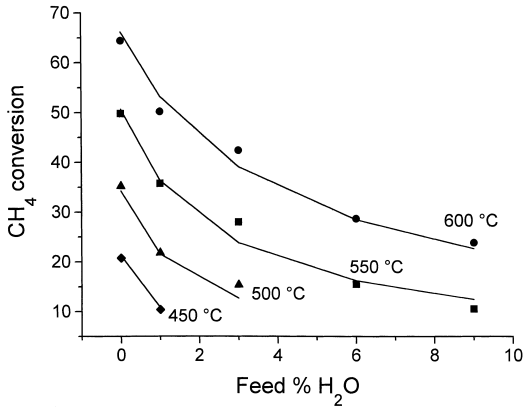

Fig. 6. Effect of water on CH_4 combustion over a PdO/γ-Al_2O_3 catalyst. Experimental data (points) vs. model prediction (lines).

This has allowed to collect several interesting indications on high temperature reaction rates which are reported in details in [31]. As one of the most prominent results, data have been obtained on the effect of water in the high temperature range. This is still a debated issue in the literature. Indeed water inhibition had been previously reported in the literature [22,23,32,33] on the basis of kinetic data collected up to 400°C. On the other hand, Dalla Betta and co-workers [33] suggested that the effect of H_2O inhibition on the ignition temperature in the range of 400–420°C is less important than expected from low temperature kinetic studies. Indeed ignition experiments performed in an adiabatic pilot scale combustor evidenced that the light-off temperature increased only from 396 to 414°C on switching the gas preheating device from an electrical heater to a diffusive burner. This latter system produced an amount of water corresponding to 1.6% (v/v) in the feed, that, according to the authors, would have resulted in a larger increase of the ignition temperature in the presence of a strong inhibition effect.

Fig. 6 reports isothermal series of CH_4 conversion data as a function of H_2O percent content in the feed. The data clearly show that H_2O strongly inhibits the reaction in all the investigated temperature range. Noteworthy at 550 and 600°C saturation is not achieved up to 9% (v/v) of H_2O

Table 2
Estimated values of kinetic parameters in the rate expression for CH_4 combustion over the 10% $PdO/\gamma\text{-}Al_2O_3$ catalyst, Eq. (14)

K'_r at 773 K = 1.2 m^3/kg/s	E_{att} = 63.6 kJ/mol
K_{H_2O} at 773 K = 5.00 m^3/mol	$\Delta H_{H_2O} = -20.8$ kJ/mol

in the feed, possibly due to the high reaction temperature. Accordingly results of Dalla Betta and co-workers [34] are likely not associated with a minor H_2O inhibition effect at high temperature, but should be reinterpreted by properly considering the strong sensitivity of adiabatic ignition to the inlet temperature.

Lines in Fig. 6 show that experimental data are nicely fitted by a simple pseudo-homogeneous isothermal plug-flow model of the structured reactor using the following rate expression, similar to that adopted in the design analysis, with parameters reported in Table 2.

$$R'_w = \left(\frac{K'_r C_{CH_4}}{1 + K_{H_2O} C_{H_2O}} \right) \text{ (mol/kg s)} \quad (14)$$

Eq. (14) also includes the effects of CH_4 (first-order) and O_2 (zeroth-order) concentration observed in the complete kinetic study [31]. On the other hand, the experimental data could not be adequately fitted using the simple power law expressions with -1 reaction order in H_2O concentration typically proposed in the literature [22,23,33]. In particular the data with H_2O concentration below 3% were widely mismatched suggesting that, in the temperature range herein considered, inhibition due to water adsorption is not so strong to originate a constant negative reaction order under all the investigated conditions.

3.3. CO oxidation in the plate-type metallic reactor

3.3.1. Thermal behavior

In the following section we address the application of a second structured system, namely the "high conductivity" plate-type reactor, to the kinetic study of catalytic combustion reactions.

The factors affecting removal of the reaction heat in structured catalysts with conductive supports have been investigated theoretically [13,35] and experimentally [14] by some of us. It has been shown that the thermal behavior of such systems is influenced primarily by the intrinsic thermal conductivity of the support material and by the geometrical features of the support. Particularly, both simulation studies and experiments pointed out that exothermic reactions over plate-type catalysts with highly conductive metallic slabs (made of, e.g. Al) would significantly decrease the hot spot temperatures as compared to catalysts with thinner slabs made of less conductive metals (e.g. stainless steel), the effective heat conductivity of the structured system being in fact proportional both to the intrinsic conductivity and to the thickness of the slabs. In line with such indications, the design of the plate-type catalyst/reactor system for the present work was based on Al slabs with 0.5 mm half-thickness, in order to achieve an excellent heat removal efficiency. The goal was in fact to prove that enhanced effective thermal conductivities are helpful in covering a broader range of conditions when investigating the kinetics of strongly exothermic catalytic reactions. Accordingly, an extensive set of CO oxidation runs was performed in the metallic plate-type reactor: in such runs, the reactor feed stream consisted of 0.7–8.8% (v/v) CO in air or air/N_2 (O_2 concentration = 4–19% v/v), with feed flow rates in the range 150–9000 cm^3/min (STP) (GHSV = 2500–150000 cm^3/(g h)), always corresponding to laminar flow conditions in the catalyst channels. The catalyst temperature was varied between 105 and 450°C. The catalytic behavior in replicated runs was found nicely reproducible over a time interval of a few months. Notably, to our knowledge no other investigation of CO catalytic oxidation has been reported which covers such an extensive range of operating conditions. It is also worth mentioning that the highest feed flows are here about two orders of magnitude greater than in the case of the kinetic experiments in the annular reactor discussed in the paragraphs above.

A first series of CO combustion runs in air was specifically devoted to investigating the thermal behavior of the metallic plate-type reactor. Fig. 7a–d show temperature distributions measured in the reactor at high CO feed contents with low, intermediate and high feed flow rates. For small feed flows (Q = 150 or 200 cm^3/min, Fig. 7a, b) the temperature distribution at 100% CO conversion was essentially uniform throughout the structured catalyst, even for CO feed concentrations Y^0_{CO} as high as 8.7% (v/v), corresponding to an adiabatic temperature rise in excess of 750°C. Only limited axial T-gradients (≈15°C) became apparent at complete conversion when the feed flow was incremented to Q = 1000 cm^3/min, whereas the reactor was still isothermal with the oven at moderate conversions (Fig. 7c). For a feed flow of 5000 cm^3/min and Y^0_{CO} = 5% (v/v) (Fig. 7d), complete CO conversion resulted in axial temperature gradients up to 70°C, because of the incremented thermal load, but the temperature profiles were still flat in the case of partial conversions, such as those required for kinetic investigations.

Fig. 8 summarizes the experimental relationship between the thermal load of CO oxidation runs (i.e. the heat evolved by the reaction for given feed flow, CO feed content and conversion) and the corresponding maximum measured temperature difference between the catalyst and the reactor oven. Inspection of Fig. 8 suggests that there may be some beneficial effect of incremented flow rates in reducing the temperature differences. On neglecting this aspect, we consider as a first approximation that the slope of a straight line through the data and the origin provides an estimate of the overall resistance of the structured reactor to the removal of the reaction heat. Based on the data in Fig. 8 such an estimate is about 2.4 K/W. Due to the absence of any significant temperature gradient on the catalyst layer and its substrate plates in the direction transverse to flow, we can regard such heat transfer resistances as essentially confined to the interface

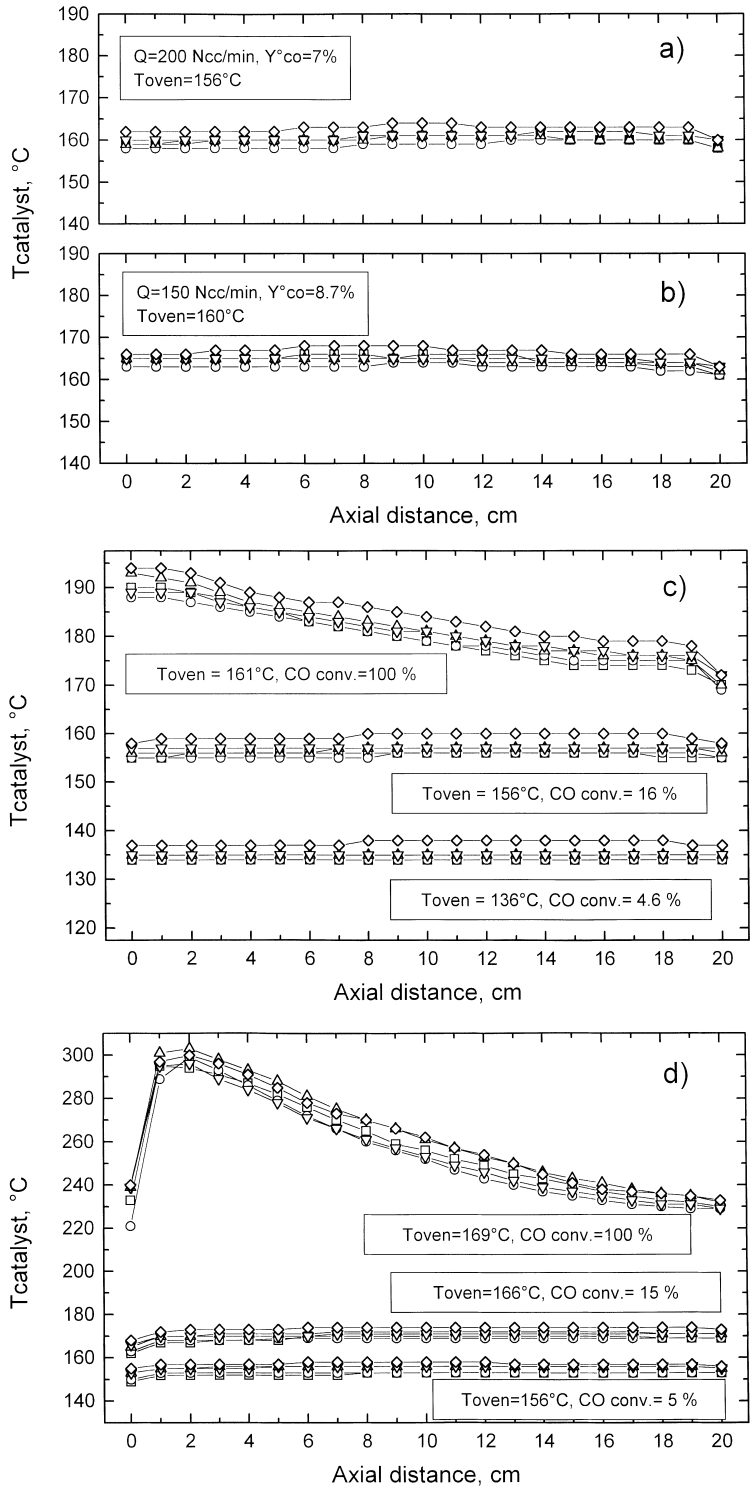

Fig. 7. Measured temperature profiles in CO combustion runs in the plate-type metallic reactor. Reaction conditions: (a) $Y^0_{CO} = 0.07$ in air, feed flow = 200 cm^3/min (STP), $T_{oven} = 156°C$, CO conversion = 100%; (b) $Y^0_{CO} = 0.087$ in air, feed flow = 150 cm^3/min (STP), $T_{oven} = 160°C$, CO conversion = 100%; (c) $Y^0_{CO} = 0.05$ in air, feed flow = 1000 cm^3/min (STP); (d) $Y^0_{CO} = 0.087$ in air, feed flow = 5000 cm^3/min (STP).

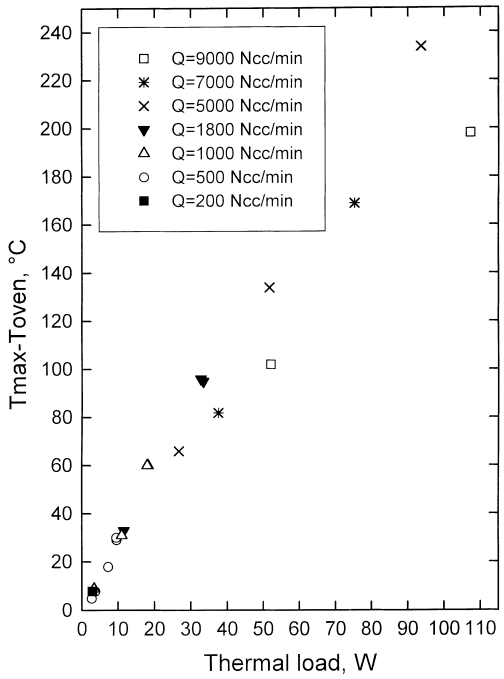

Fig. 8. Correlation between maximum catalyst over temperature and thermal load of CO combustion runs in the plate-type metallic reactor.

between the catalyst slabs and the inner wall of the reactor tube. For feed flows in excess of 2000 cm^3/min and high CO conversions, however, we noticed the onset of temperature gradients also between the outer wall of the reactor tube and the oven atmosphere, indicating that external heat transfer resistances would become significant in our experimental system in the case of such high thermal loads.

The efficiency exhibited by the metallic plate-type reactor in distributing and removing the heat of CO combustion prompted us to investigate further its potential with respect to the kinetic study of highly exothermic catalytic reactions, including catalytic combustion reactions as well as, e.g. partial oxidations of hydrocarbons.

3.3.2. Kinetic study

Previous published work on the kinetics of CO catalytic combustion is related to Pt-based three-way catalysts [36–38]. Limited feed concentrations of CO ($\leq$4 vol.%) and O_2 ($\leq$2 vol.%), as typical of automotive exhaust gases, were used in the experiments.

We present herein a kinetic study of CO oxidation in air over the 3% (w/w) Pd/γ-Al_2O_3 catalyst in the metallic plate-type reactor discussed above, which covers a very wide range of CO feed concentrations up to 8.8 vol.%, i.e. close to the lower flammability limit in air at atmospheric pressure.

During preliminary work, we found that a complete kinetic investigation of CO oxidation in air over the PdO/γ-Al_2O_3 catalyst in the form of powder loaded in a conventional flow microreactor was prevented by the onset of strong temperature gradients as soon as the CO feed content exceeded 3.5 vol.%. As mentioned before, however, in the experimental field where operation of the microreactor was feasible, we noticed a substantial agreement with the catalytic activity data obtained in the plate-type reactor with slabs coated by the same PdO/γ-Al_2O_3 catalyst: accordingly, testing the catalyst in the form of a washcoat deposited onto Al slabs provides data which can be regarded as representative of intrinsic catalytic kinetics.

Fig. 9 shows CO conversion data measured in CO oxidation with air for a given CO feed content: they are plotted versus the maximum catalyst temperature for different feed flow rates. Fig. 10 illustrates the effect of varying the CO feed content at a fixed feed flow rate. The PdO/γ-Al_2O_3 coating resulted fairly active in CO combustion, with a light-off temperature markedly increasing with increasing feed concentration of CO. This behavior corresponds to a negative reaction order with respect to CO, in line with previous reports on the kinetics of CO oxidation over noble metal catalysts [36,37]. On the other hand, no significant effect of CO_2 was detected during dedicated runs with up to 8% (v/v) carbon dioxide added to the feed.

A more detailed kinetic study was then addressed. The goal was the development of a suitable rate expression in view of its later inclusion into a mathematical model of the structured reactor, by which the thermal behavior of our coated plate-type systems could be analyzed. The adopted empirical form of the rate expression, Eq. (15), was based on literature kinetic studies of CO oxidation over noble-metal catalysts [36–38]:

$$R_{CO} = \frac{k_1 p_{CO} p_{O_2}^{1/2}}{(1 + K_{CO} p_{CO})^2} \text{ (mol/kg s)} \quad (15)$$

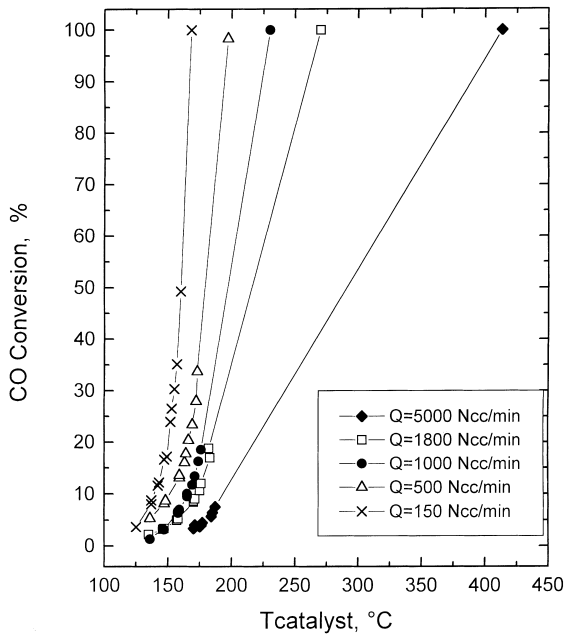

Fig. 9. CO combustion runs in air, plate-type metallic reactor. Influence of catalyst temperature and feed flow rate on CO conversion. $Y^0_{CO} = 0.087$.

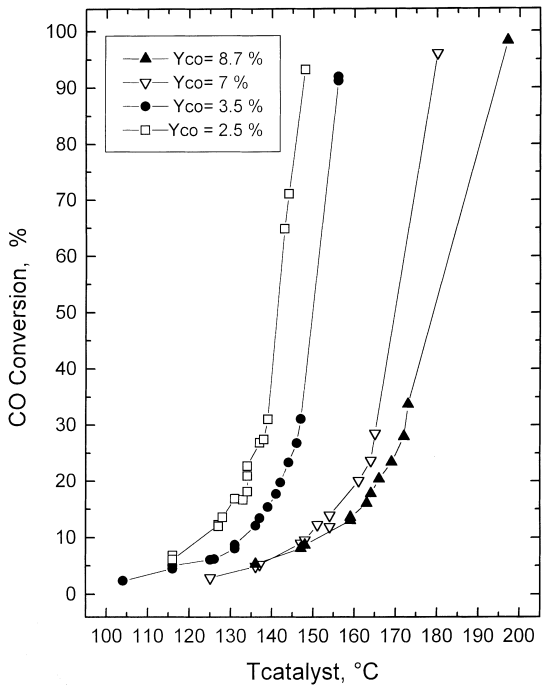

Fig. 10. CO combustion runs in air, plate-type metallic reactor. Influence of catalyst temperature and CO feed concentration on CO conversion. Feed flow rate = 500 cm^3/min (STP).

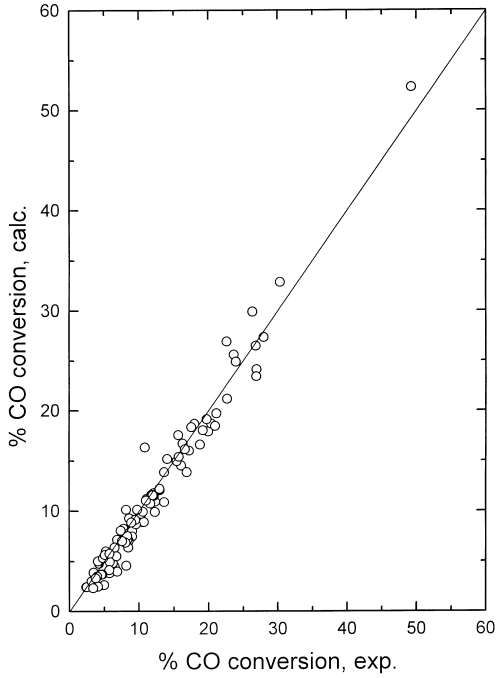

Fig. 11. Parity plot for the kinetic analysis of CO combustion in the plate-type metallic reactor.

Eq. (15) includes two kinetic parameters, namely the rate constant k_1 and the pseudo-adsorption constant K_{CO}: their estimates, along with their temperature dependence, were determined by nonlinear regression on integral data from 100 CO oxidation runs, with CO percent conversion as the experimental response, using a simple pseudo-homogeneous isothermal plug-flow model of the structured reactor. The data covered the effects of temperature, feed flow and inlet feed concentrations of CO and O_2. Only runs with less than 5°C difference between maximum and minimum catalyst temperature readings were considered.

Table 3 provides the estimates of the four rate parameters. A strong correlation affecting the four estimates prevents discussion of their individual values. The overall adequacy of the fit is documented by the comparison of experimental data with model predictions in the parity plot of Fig. 11. The average absolute error of the fit was 1.163; the average percent error was 11.6, which well compares with the experimental uncertainty of the CO conversion measurements.

The significance of gas/solid (interphase) mass transfer limitations in the plate-type reactor was ruled out a posteriori based on the evaluation of the following Damkohler number:

Table 3
Estimated values of kinetic parameters in the rate expression for CO combustion over the 3% $PdO/\gamma Al_2O_3$ catalyst, Eq. (15)

k_1 at 473 K = 27.7 mol/kg/s/$bar^{3/2}$	E_{att} = 36.9 kJ/mol
K_{CO} at 473 K = 84.8 bar^{-1}	ΔH_{CO} = −39.9 kJ/mol

$$Da = \frac{R_{CO} d_h}{D_{CO} C_{CO}} \tag{16}$$

In Eq. (16), d_h represents the hydraulic diameter of the channels in the plate-type catalyst, i.e. twice the spacing between slabs. The diffusivity of CO in air at temperature (T) was evaluated according to

$$D_{CO} = D^0_{CO} \left(\frac{T}{T_0} \right)^{1.75} \tag{17}$$

with D^0_{CO} = 0.32 cm^2/s = molecular diffusivity of CO in air at T_0 = 373 K [22]. It was found that $Da \ll 0.1$ under the conditions considered for the kinetic analysis. This indicates that the rate of gas/solid mass transfer in the channels of the plate-type catalyst was always much greater than the rate of reaction, so that external diffusional limitations could be safely neglected.

The role of intraporous diffusion was evaluated by means of the following dimensionless group, representative of the ratio between the observed rate of reaction and the rate of internal diffusion:

$$\Phi^2 = \frac{R_{CO} \delta_w}{D^e_{CO} C_{CO}} \tag{18}$$

An order-of-magnitude estimate of 10^{-6} m^2/s was used for D^e_{CO}. It was found that $\Phi \ll 0.1$ under all the conditions of the kinetic runs, which indicates the negligible effects of intraporous diffusional limitations.

On the basis of the parameter estimates in Table 3, the average reaction order with respect to CO was negative in

the range $Y^0_{CO} = 0.01$–0.09, and approached -1 at the highest CO feed contents. This further confirms the absence of diffusional intrusions.

Rate (Eq. (15)) was successfully applied to the kinetic analysis of CO oxidation over other structured catalysts samples with Pd/Al_2O_3 washcoats. It was also included in a nonisothermal model of the metallic plate-type reactor, by which an engineering analysis of the thermal behavior of such a reactor was carried out [14].

4. Conclusions

The experimental and theoretical results presented in this paper have demonstrated specifically designed structured catalytic reactors as effective tools for kinetic investigation of catalytic combustion reactions under severe conditions.

The following major advantages have been pointed out:

- the parallel flow pattern guarantees negligible pressure drop with high flow rates, so that tests with extremely high GHSV can be performed to investigate kinetics of ultra-fast reactions under conditions representative of their industrial application;
- the regular geometry allows one to define accurately the fluid dynamics and particularly the gas/solid contact, even in the case of catalyst loads of a few milligrams which can be hardly handled in conventional packed bed reactors; this can be exploited for reliable reactor design and analysis by mathematical modeling;
- the impact of diffusion processes can be minimized through reactor design combined with appropriate coating techniques;
- an effective dissipation of reaction heat can be achieved through different mechanisms (radiation, convection and conduction), which are typically not available in conventional packed-bed reactors;
- the procedures followed for the preparation of the investigated structured catalysts, which are obtained by deposition of active catalytic layers onto ceramic or metallic supports, closely resemble those adopted for production of industrial monolith catalysts, which guarantees the practical significance of the kinetic data.

The annular reactor configuration provides a good example of how such advantages can be combined into a device that can be manufactured in a very small scale with conventional laboratory techniques and materials. In those cases where dissipation of the reaction heat becomes the critical issue, the plate-type metallic reactor can represent a valuable solution.

Acknowledgements

Financial support for this work was provided by MURST Rome, Italy and by Japan Cooperation Center Petroleum Tokyo, Japan.

References

[1] G. Groppi, P. Forzatti, Catalytic combustion for the production of energy, Catal. Today 54 (1999) 165.
[2] R.A. Dalla Betta, N. Ezawa, K. Tsurumi, J.C. Schlatter, S.G. Nickolas, Two stage process for combusting fuel mixtures, US Patent 5183401 (1993).
[3] R.A. Dalla Betta, K. Tsurumi, N. Ezawa, Multistage process for combusting fuel mixtures using oxide catalyst in the hot stage, US Patent 5232257 (1993).
[4] P. Evans, First commercial XONON specified for a GE 7FA, Modern Power Systems, March 2000, p. 27.
[5] S. Ro, A. Scholten, Catalytic combustion in a domestic natural gas burner, Catal. Today 47 (1999) 415.
[6] I. Cerri, G. Saracco, F. Geobaldo, V. Specchia, Development of a methane premixed catalytic burner for household applications, Ind. Eng. Chem. Res. 39 (2000) 24.
[7] A. Scholten, R. Van Yperen, J. Emmerzaal, A Zero NO_x Catalytic Ceramic Natural Gas Cooker, Book of Abstract, in: Proceedings of the 4th IWCC, San Diego, USA, April 14–16, 1999, p. 35.
[8] G. Groppi, E. Tronconi, P. Forzatti, Mathematical models of catalytic combustors, Catal. Rev. Sci. Eng. 41 (1999) 227.
[9] S.T. Kolaczkowski, Catalytyc stationary gas turbine combustors: a review of the challanges faced to clear the set of hurdles, Trans. I. Chem. Eng. Part A 73 (1995) 168.
[10] J. McCarty, Kinetics of PdO combustion catalysts, Catal. Today 26 (1995) 283.
[11] E.M. Johansonn, S.G. Jaras, Circumventing fuel NO_x formation in catalytic combustion of gasified biomasses, Catal. Today 47 (1999) 359.
[12] A. Beretta, P. Baiardi, D. Prina, P. Forzatti, Analysis of a catalytic annular reactor for very short contact times, Chem. Eng. Sci. 54 (1999) 765.
[13] G. Groppi, E. Tronconi, Design of novel monolith honeycomb catalyst support for gas/solid reaction with heat exchange, Chem. Eng. Sci. 55 (2000) 2161.
[14] E. Tronconi, G. Groppi, A study on the thermal behavior of structured plate-type catalysts with metallic supports for gas–solid exothermic reactions, Chem. Eng. Sci., 2000, in press.
[15] S. Yasaki, Y. Yoshino, K. Ihara, K. Ohkubo, Method of manufacturing an exhaust gas purifying catalyst, US Patent 5208206 (1993).
[16] R.A. Dalla Betta, T. Shoij, K. Tsurumi, N. Ezawa, Catalyst structure having integral heat exchange, US Patent 5250489 (1993).
[17] R.A. Dalla Betta, F.H. Ribeiro, T. Shoij, K. Tsurumi, N. Ezawa, S.G. Nickolas, Partial combustion process and a catalyst structure for use in the process, US Patent 5326253 (1994).
[18] S. Soled, γ-Al_2O_3 viewed as a defect oxyhydroxide, J. Catal. 81 (1983) 252.
[19] G. Groppi, C. Cristiani, M. Valentini, E. Tronconi, Development of novel structured catalytic reactors for highly exothermic reactions, Studies Surf. Sci. Catal. 130 (2000) 2747.
[20] B. Finlayson, Nonlinear Analysis in Chemical Engineering, McGraw Hill, New York, 1980.
[21] T.C. Wayburn, J.D. Seader, Homotopy continuation methods for computer-aided process design, Comp. Chem. Eng. 11 (1987) 7.
[22] K. Fujimoto, F.H. Ribeiro, M. Avalos-Borja, E. Iglesia, Structure and reactivity of PdO_x/ZrO_2 catalysts for methane oxidation at low temperature, J. Catal. 179 (1999) 431.
[23] J.C. Van Giezen, F.N. Van Den Berg, J.L. Kleinen, A.J. Van Dillen, J.W. Geus, The effect of water on the activity of supported palladium catalysts in the catalytic combustion of methane, Catal. Today 47 (1999) 287.
[24] R.C. Reid, J.M. Prausnitz, B.E. Poling, The Properties of Gases and Liquids, 4th, Edition, McGraw-Hill, New York, 1987.
[25] S. Irandoust, B. Andersson, Monolith catalysts for nonautomobile applications, Catal. Rev. Sci. Eng. 30 (1988) 341.

[26] N. Wakao, J. Smith, Diffusion in catalyst pellets, Chem. Eng. Sci. 17 (1962) 825.
[27] R.K. Shah,. A.L. London, Laminar Flow Forced Convection, Academic Press, New York, 1978.
[28] M.T. Janicke, H. Kestenbaum, U. Hagendorf, F. Schuth, M. Fichtner, K. Schubert, The controlled oxidation of hydrogen from an explosive mixture of gases using a microstructured reactor/heat exchanger and Pt/Al_2O_3 catalyst, J. Catal. 191 (2000) 282.
[29] A. Beretta, G. Groppi, L. Majocchi, P. Forzatti, Potentialities and drawbacks of the experimental approach to the study of high-T high GHSV kinetics, Appl. Catal. A: Gen. 187 (1999b) 49.
[30] W. Ibashi, G. Groppi, P. Forzatti, in preparation.
[31] G. Groppi, W. Ibashi, M. Valentini, P. Forzatti, High temperature combustion of CH_4 over PdO/Al_2O_3: kinetic measurements in a structured reactor, Chem. Eng. Sci., 2000, in press.
[32] C.F. Cullis, T.G. Nevell, D.L. Trimm, Role of the catalyst support in the oxidation of methane over palladium, J. Chem. Soc. Faraday Trans. 1 (1971) 1406.
[33] F.H. Ribeiro, M. Chow, R.A. Dalla Betta, Kinetics of the complete oxidation of methane over supported palladium catalysts, J. Catal. 146 (1994) 537.
[34] R.A. Dalla Betta, J.C. Schlatter, D.K. Yee, D.G. Loffler, T. Shoji, Catalytic combustion technology to achieve ultralow NO_x emissions: catalyst design and performances characteristics, Catal. Today 26 (1995) 329.
[35] G. Groppi, E. Tronconi, Continuous versus discrete models of nonadiabatic monolith catalysts, AIChE J. 42 (1996) 2382.
[36] S.E. Voltz, C.R. Morgan, B.A. Liederman, Kinetic study of carbon monoxide and propylene oxidation on platinum catalysts, Ind. Eng. Chem. Proc. Des. Dev. 12 (1973) 294.
[37] B. Subramanian, A. Varma, Reaction kinetics on a commercial three-way catalyst: the $CO–NO–O_2–H_2O$ system, Ind. Eng. Chem. Proc. Des. Dev. 24 (1985) 512.
[38] C. Dubien, D. Schweich, G. Mabilon, B. Martin, M. Prigent, Three-way catalytic converter modelling: fast- and slow-oxidizing hydrocarbons, inhibiting species, and steam reforming reaction, Chem. Eng. Sci. 53 (1998) 471.